

Comment

This manuscript was not published eventually, for two reasons:

- The findings were too similar to the localization of wrinkles obtained earlier for a sheet on an elastic foundation. See G. W. Hunt, M. K. Wadee, and N. Shia-colas, J. Appl. Mech. **60**, 1033 (1993). Note, however, that the two problems are not equivalent. For an elastic foundation the second term in the energy density, eq. (1), is $(K/2)h^2$ rather than $(K/2)h^2 \cos \phi$.
- We have found the exact solution to the problem presented here. See arXiv:1107.5505.

In addition, B. Audoly has followed this preprint to show, using an amplitude-equation approach, that the variational *Ansatz* used here is indeed the profile minimizing the energy to quartic terms in the height amplitude. See B. Audoly, Phys. Rev. E **84**, 011605 (2011). This article also presents a unified perturbative treatment for several types of substrate, including the fluid substrate and the linear elastic foundation.

If you find the manuscript useful nonetheless, and wish to cite it, please use arXiv:1009.2487.

Instability of infinitesimal wrinkles against folding

Haim Diamant¹ and Thomas A. Witten²

¹ Raymond and Beverly Sackler School of Chemistry, Tel Aviv University, Tel Aviv 69978, Israel; e-mail: hdiament@tau.ac.il

² Department of Physics and James Franck Institute, University of Chicago, Chicago, Illinois 60637, USA; e-mail: t-witten@uchicago.edu

February 23, 2024

Abstract. We analyze the buckling of a rigid thin membrane floating on a dense fluid substrate. The interplay of curvature and substrate energy is known to create wrinkling at a characteristic wavelength λ , which localizes into a fold at sufficient buckling displacement Δ . By analyzing the regime $\Delta \ll \lambda$, we show that wrinkles are unstable to localized folding for *arbitrarily small* Δ . After observing that evanescent waves at the boundaries can be energetically favored over uniform wrinkles, we construct a localized *Ansatz* state far from boundaries that is also energetically favored. The resulting surface pressure P in conventional units is $2 - (\pi^2/4)(\Delta/\lambda)^2$, in entire agreement with previous numerical results. The decay length of the amplitude is $\kappa^{-1} = (2/\pi^2)\lambda^2/\Delta$. This case illustrates how a leading-order energy expression suggested by the infinitesimal displacement can give a qualitatively wrong configuration.

PACS. XX.XX.XX No PACS code given

1 Introduction

Recent work has revealed a wealth of spontaneous spatial structures in thin elastic sheets, owing to their easy deformability by bending [1, 2, 3, 4, 5, 6, 7, 8, 9, 10, 11, 12, 13, 14, 15]. Special interest has focussed on the recently-proposed wrinkle-to-fold transition in compressed thin sheets floating on a dense liquid [10]. Such composite structures occur widely in industrial coatings and biological tissues. The sheet can be a 50-nm-thick metal film [8] or a two-nanometer-thick lipid monolayer [9].

When compressed to the point of buckling, the incipient deformation is an undulation or wrinkle whose wavelength λ is a combination of the bending stiffness and the substrate rigidity, as specified below. A compressional displacement Δ accompanies this buckling. Buckling occurs when the compressional force per unit length P exceeds a threshold. In the conventional units defined below, this threshold P is equal to 2. As with the classic Euler buckling of a compressed rod [16], the buckled structure is unstable under this force: larger displacement creates more bending deflection, which requires a smaller pressure. Thus P decreases as Δ increases.

For sufficiently large Δ of order λ , the weak-deflection expression for the energy becomes inadequate, and the selected structure is no longer a uniform undulation but a localized fold. Reference [10] explored the transition from the wrinkled to the folded state numerically and experimentally, concluding that the transition occurs for $\Delta \simeq \lambda/3$. They determined numerically that the dimensionless force P is well represented as $2 - 2.47(\Delta/\lambda)^2$. As Δ

decreases, the buckled region was observed to be less and less localized, and to span more and more wavelengths, eventually spanning the system.

These observations led us to consider the regime of indefinitely small displacements $\Delta \ll \lambda$, in order to discern how the corrections to the small-deformation energy emerge. As explained below, we found that these corrections remain important even for arbitrarily small displacements. The resulting buckling pattern is always localized, though its spatial extent diverges as the displacement Δ decreases to zero. Since the regime of small displacements is analytically tractable, we could obtain a closed-form expression for the $P(\Delta)$ function: $P = 2 - (\pi^2/4)(\Delta/\lambda)^2 + \mathcal{O}((\Delta/\lambda)^4)$. This agrees completely with the numerical value cited above. We also obtain a closed-form expression for the buckling profile in this regime. Though this form is obtained by a variational *Ansatz*, we argue below that it approaches the exact profile in the limit of small displacement.

2 Model

We consider a two-dimensional problem of a thin incompressible elastic sheet of length L , width W , and bending modulus B . The sheet is assumed to deform in the xz plane while remaining uniform along the y axis. Being incompressible, its total length L is fixed, and its configuration, including the total displacement along the x axis, Δ , is fully accounted for by a height profile, $h(s)$, as a function of arclength $s \in [-L/2, L/2]$. The region $z < h$

is occupied by a liquid of mass density $\rho = K/g$ (g being the gravitational acceleration). See fig. 1.

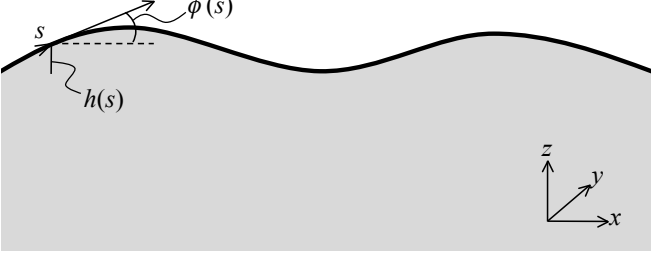


Fig. 1. Schematic view of the system and its parametrization.

For a certain configuration, $h(s)$, the energy of the sheet E and the displacement Δ are given by

$$\begin{aligned} E &= W \int_{-L/2}^{L/2} ds \left(\frac{1}{2} B \dot{\phi}^2 + \frac{1}{2} K h^2 \cos \phi \right), \\ \Delta &= \int_{-L/2}^{L/2} ds (1 - \cos \phi), \end{aligned} \quad (1)$$

where $\phi(s)$ is the angle between the local tangent to the sheet and the x axis at arclength s (cf. fig. 1), and a dot denotes a derivative with respect to s . It is helpful to work in units where $B = K = 1$, *i.e.*, rescale the energy by B and all lengths by $(B/K)^{1/4}$. The pressure P is then scaled by $(BK)^{1/2}$. We shall also let $W = 1$ in what follows. Using these definitions and the geometrical relation $\dot{h} = \sin \phi$, we rewrite eq. (1) as

$$\begin{aligned} E &= \frac{1}{2} \int_{-L/2}^{L/2} ds \left(\frac{\dot{h}^2}{1 - \dot{h}^2} + h^2 \sqrt{1 - \dot{h}^2} \right), \\ \Delta &= \int_{-L/2}^{L/2} ds \left(1 - \sqrt{1 - \dot{h}^2} \right). \end{aligned} \quad (2)$$

Our aim is to find the height profile, $h(s)$, which minimizes the energy of the sheet for a given displacement Δ , $E = E^*(\Delta)$; from this we may find the resulting pressure–displacement relation, $P(\Delta) = dE^*/d\Delta$.

3 Extended wrinkling

Let us substitute in eq. (2) a uniformly wrinkled height profile of amplitude A and wavenumber k ,

$$h(s) = A \cos(ks). \quad (3)$$

The extensivity of the energy implies that $E = L\mathcal{E}(\delta)$ with $\delta = \Delta/L$. To second order in A^2 we get

$$\mathcal{E} = \frac{1}{4}(k^4 + 1)A^2 + \frac{1}{32}k^2(2k^4 - 1)A^4, \quad (4)$$

$$\delta = \frac{1}{4}k^2A^2 + \frac{3}{64}k^4A^4. \quad (5)$$

We first examine the leading order. Substituting eq. (5) in eq. (4) yields $\mathcal{E}(\delta) = (k^2 + k^{-2})\delta$. For any $\delta > 0$ the energy has a minimum of $\mathcal{E}^* = 2\delta$ for $k = 1$. This marks the linear wrinkling instability [17, 3, 18], with a finite wavenumber $k_c = 1$ [wavelength $\lambda = 2\pi(B/K)^{1/4}$], squared amplitude $A^2 = 4\delta$, and energy $E^* = 2\Delta$. The resulting critical pressure is $P_c = dE^*/d\Delta = 2$.

Repeating the same procedure in the next order, we find from eqs. (4) and (5)

$$\mathcal{E}(\delta) = (k^2 + k^{-2})\delta + (k^2 - 5k^{-2})\delta^2/4. \quad (6)$$

This expression is still minimized by $k = k_c = 1$, yielding $\mathcal{E}^*(\delta) = 2\delta - \delta^2$, *i.e.*,

$$\begin{aligned} E^*(\Delta) &= 2\Delta - \Delta^2/L \\ P(\Delta) &= 2 - 2\Delta/L. \end{aligned} \quad (7)$$

4 Localized folding

While the solution to the leading-order problem must be of the wrinkling form [eq. (3)], such an extended profile does not necessarily minimize the anharmonic energy. Indeed, the next-leading energy correction in eq. (7) vanishes as $L \rightarrow \infty$; the wrinkle profile gains no energetic benefit from this correction in the infinite system.

To see that a localized solution should be favorable, let us fix the pressure (rather than the displacement) at a value slightly below threshold, $P = 2 - p$ with $0 < p \ll 1$, and re-examine the leading-order problem. The energy to be minimized in this case is $\mathcal{G} = \mathcal{E} - P\delta \simeq A^2(k^4 - Pk^2 + 1)/4$, where we have used the leading order in eqs. (4) and (5). The most favorable wrinkling profile has $k^2 = 1$ and $\mathcal{G} = (A^2/4)p > 0$, which is larger than $\mathcal{G} = 0$ of the flat state. Thus, the flat state is linearly stable against wrinkling for $P < P_c$. Nonetheless, we can get a lower energy if we allow for a complex wavenumber. We may obtain $\mathcal{G} = 0$ by taking

$$k \simeq 1 \pm i\kappa, \quad \kappa = \sqrt{p}/2. \quad (8)$$

Hence, according to the leading-order theory, if there were a boundary at $s = 0$, an ‘evanescent wave’ adjacent to the boundary, of the form $h(s > 0) = Ae^{is - \kappa s}$, could be stabilized for $P < P_c$. For such a fixed pressure the flat state is linearly stable against wrinkling, and a ‘propagating wave’ can be stabilized strictly at $P = P_c$.

We are interested, however, in profiles which are localized far away from boundaries. Accordingly, we seek a wave-packet profile with a spectral content similar to the evanescent-wave profile above. One such profile is

$$h(s) = A \frac{\cos(ks)}{\cosh(\kappa s)}, \quad (9)$$

where the decay coefficient κ is used as a variational parameter, and we take $k = k_c = 1$. (Letting k be another variational parameter does not change the results.) We assume the limit $L^{-1} \ll \kappa \ll k = 1$, where the wavy profile is ‘underdamped’ but decays sufficiently fast for the

system size to be taken as infinite. The extensivity of the energy again implies $E = \kappa^{-1}\mathcal{E}(\delta)$, where now $\delta = \kappa\Delta$. As in the preceding section we perform the calculation to order δ^2 ; yet, unlike the extended-wrinkling case, the result will be of higher order in Δ , since the domain size itself, κ^{-1} , depends on Δ .

Substituting eq. (9) in eq. (2), we obtain within the assumed order of approximation,

$$\mathcal{E} = (1 + \kappa^2)A^2 + \frac{1}{24}A^4 \quad (10)$$

$$\delta = \frac{1}{6}(3 + \kappa^2)A^2 + \frac{1}{16}A^4. \quad (11)$$

Solving eq. (11) for A^2 ,

$$A^2 = 2(1 - \kappa^2/3)\delta - \delta^2/2, \quad (12)$$

and substituting it back in eq. (10), we get $\mathcal{E}(\delta) = 2(1 + 2\kappa^2/3)\delta - \delta^2/3$. To properly minimize the energy with respect to κ for fixed Δ , we rewrite this result as

$$E = 2(1 + 2\kappa^2/3)\Delta - \kappa\Delta^2/3.$$

As expected, to the leading order the energy is minimum for $\kappa = 0$ and coincides with that of the wrinkling case, $E^* = 2\Delta$. However, with the anharmonic term the energy is minimized by $\kappa = \Delta/8$, yielding

$$\begin{aligned} E^*(\Delta) &= 2\Delta - \frac{\Delta^3}{48} \\ P(\Delta) &= 2 - \frac{\Delta^2}{16}. \end{aligned} \quad (13)$$

Note that the result $\kappa = \Delta/8 = \sqrt{2 - P}/2$ is identical to the one obtained for the evanescent wave from the leading-order problem, eq. (8).

Finally, substituting $\kappa = \Delta/8$ back in eqs. (12) and (9), we obtain for the localized profile,

$$h(s) = \frac{\Delta}{2} \left(1 - \frac{7\Delta^2}{384} \right) \frac{\cos s}{\cosh[(\Delta/8)s]}. \quad (14)$$

Equations (13) and (14) are our central results. Comparing the energies of the extended and localized profiles, eqs. (7) and (13), we find that the localized fold is stabilized for $\Delta > \Delta_c = 48/L$. Thus, the wrinkle-to-fold transition presented in ref. [10] is a finite-size effect; in the limit $L \rightarrow \infty$ the deformation of the sheet is always localized in a folded domain of negligible width compared to the system size, $\kappa^{-1} = 8/\Delta$ [or, in dimensional terms, $\kappa^{-1} = (2/\pi^2)\lambda^2/\Delta$]. The parabolic pressure-displacement relation of eq. (13) is rewritten in dimensional terms as

$$\frac{P}{(BK)^{1/2}} = 2 - \frac{\pi^2}{4} \left(\frac{\Delta}{\lambda} \right)^2,$$

which agrees nicely with the numerical result of ref. [10], $P/(BK)^{1/2} \simeq 2 - 2.47(\Delta/\lambda)^2$.

From eqs. (7) and (13) one might conclude that the appearance of the localized state at $\Delta = \Delta_c$ is a first-order

transition with discontinuous jumps in κ and P . This is an artifact, arising from the assumption $\kappa^{-1} \ll L$, which breaks down for $\Delta \sim \kappa \sim L^{-1}$. As shown in the Appendix, a more careful analysis for such small displacements yields a second-order transition, with $\kappa = 0$ for $\Delta < \Delta_c$ and $\kappa \sim (\Delta - \Delta_c)^{1/2}$ for $\Delta > \Delta_c$, leading to a discontinuous jump in $dP/d\Delta$.

5 Numerical solution

The calculations given in sects. 3 and 4 are valid sufficiently close to the instability. To examine the deformation of the sheet at larger displacements we derive the Euler-Lagrange equation, corresponding to the minimization of E for a given Δ , and solve it numerically.

We would like to find the profile $h(s)$ that minimizes the elastic energy E under the constraint of fixed displacement Δ , where $E[h(s)]$ and $\Delta[h(s)]$ have been defined in eq. (2). The following equation is obtained from calculating the variation of $G = E - P\Delta$ with respect to $h(s)$ and setting it to zero:

$$\begin{aligned} (1 - \dot{h}^2)^2 \ddot{h} + 4(1 - \dot{h}^2)\dot{h}\ddot{h} + (1 + 3\dot{h}^2)\ddot{h}^3 \\ + (h^2/2 + P)(1 - \dot{h}^2)^{3/2}\ddot{h} + h(1 - \dot{h}^2)^{5/2} = 0. \end{aligned} \quad (15)$$

This equation needs to be supplemented by four boundary conditions, for example, the hinge conditions $h(\pm L/2) = 0$ and $\dot{h}(\pm L/2) = 0$.

In the following examples we look for even profiles, $h(-s) = h(s)$, over a system length of $L = 21\pi$ (*i.e.*, containing $10\frac{1}{2}$ wrinkling wavelengths). For a given $P < P_c = 2$, eq. (15) is solved numerically over the interval $s \in (-L/2, 0)$ using the following boundary conditions: $h(-L/2) = 0$, $\ddot{h}(-L/2) = 0$, $\dot{h}(0) = 0$, $h(0) = h_0$. We shoot for the value of h_0 so as to make $|\dot{h}(0)|$ vanish within the required accuracy. Once $h(s)$ is found, the displacement $\Delta(P)$ is calculated using eq. (2). The results are presented in fig. 2, where they are compared with the analytical ones, eqs. (13) and (14).

The discrepancy between the numerically determined height profile and the theoretical one is of the order of a few percent, up to about 10%. It increases with Δ as expected [fig. 2(a)]. The predicted parabolic law for $P(\Delta)$, however, agrees with the numerics to a much greater extent [fig. 2(b)]. The agreement is remarkable for large displacements, where the perturbative theory is not expected to hold at all. Since we have carried out the analytical calculation to order δ^2 , we should have expected a correction to E of order $\kappa^{-1}\delta^3 \sim \Delta^5$, leading to a correction of order Δ^4 in P . Even for nearly vertical deflections (right side of fig. 3) the discrepancy is consistent with numerical error. The large discrepancies at small Δ come from the finite- L effect discussed above. This effect should become exponentially small in $\kappa L \sim L\Delta$, which explains the sharp decay of the discrepancy σ_Δ with Δ and its strong dependence on L . [See fig. 2(b) inset.] We have replotted in fig. 3 the data of that inset as a function of $\kappa L = (\Delta/8)L$ on a semi-logarithmic scale, confirming the exponential decay of the

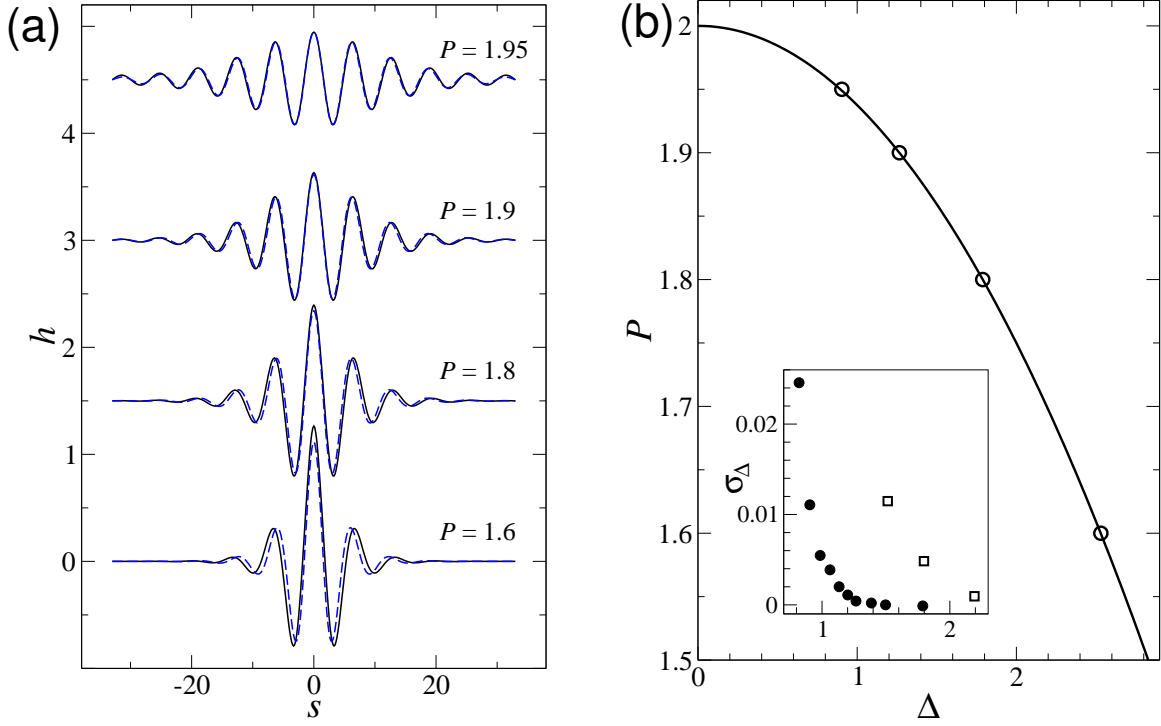


Fig. 2. (a) Height profiles obtained from the numerical solution (black solid curves) and the approximate theory [eq. (14), blue dashed curves]. Different curves correspond (from top to bottom) to decreasing pressure (as indicated) and increasing displacement. The length is $L = 21\pi$. Consecutive curves are vertically shifted by 1.5 for clarity. Note that the profiles are presented in terms of the material coordinate s rather than the projected coordinate x . (b) Pressure as a function of displacement. The open circles are the numerical values obtained from the profiles shown in (a). The solid curve is the theoretical prediction [eq. (13)]. The inset shows the normalized discrepancy σ_Δ between our numerical $\Delta(P)$ and that of eq. (13); specifically, $\sigma_\Delta \equiv (\Delta_{\text{num}} - \Delta_{\text{th}})/\Delta_{\text{num}}$. Solid circles are for $L = 21\pi$; open squares are for $L = 11\pi$.

discrepancy with κL . We note that the numerical results presented in ref. [10] seem to indicate that the parabolic pressure–displacement relation remains accurate up to the point of self-contact. All of the above suggests that $P(\Delta)$ of eq. (13) might, in fact, be the *exact* relation in the limit $\kappa L \gg 1$.

6 Discussion

In this section we argue that for the limit of small amplitude our *Ansatz* should become exact. We discuss the meaning of the simple large-amplitude behavior noted above. We comment on the relevance of our result for recent Langmuir buckling observations. We draw parallels to other continuous instabilities that are not predicted by lowest-order perturbation of the energy function.

Figure 2 shows a near match between the numerically determined profile and the *Ansatz* of eq. (9). The agreement becomes better as the threshold is approached. In this limit our asymptotic $\mathcal{O}(A^4)$ energy becomes accurate. Further, the spectral profile of eq. (9) approaches that of the evanescent wave that minimizes this asymptotic energy. This profile has a peak at $k = 1$ of width κ . The

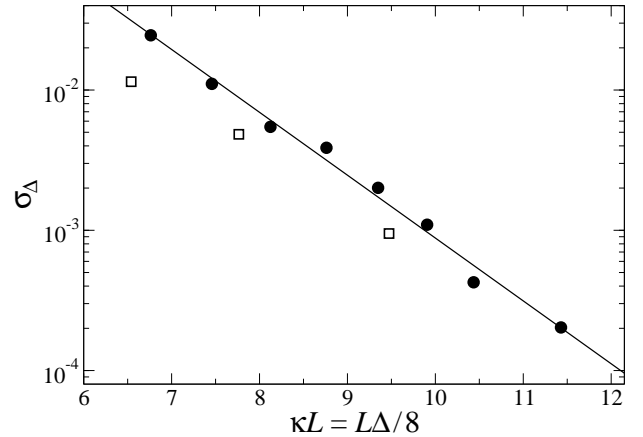


Fig. 3. Discrepancy between theory and numerics as a function of $\kappa L = (\Delta/8)L$ for $L = 21\pi$ (solid circles) and $L = 11\pi$ (open squares) on a semi-logarithmic scale. The fitted line has a slope of -1.03 ± 0.04 .

profile of eq. (9) has a spectral weight that falls off exponentially for $k - 1 \gg \kappa$. We expect that any *Ansatz* with such a spectral distribution would approach the actual profile near the threshold. However, not any profile

with the proper width and peak position is adequate. One such profile is $h(s) = A \sin s e^{-\kappa|s|}$. This profile gives the same qualitative behavior of the energy and pressure for a given displacement Δ as eq. (9), yet, here the spectral weight falls off as a power of $k - 1$, rather than the exponential falloff of eq. (9). Accordingly, we found that its energy is fractionally larger than that of eq. (9).

Our *Ansatz* is not unique. For example, the alternative form

$$h(s) = A \cos(ks) / \cosh^2(\kappa s/2)$$

has the same spectral features noted for eq. (9). However, neither profile is exact; thus when expanded in powers of Δ , both must differ from the true behavior in some order. For example, the $(7/384)\Delta^2$ correction in eq. (14) depends on our choice of *Ansatz*.

The theory predicts a quadratic initial dependence of pressure on displacement, as reported already in ref. [10]. As noted above, the quadratic dependence remains accurate far beyond the small-displacement regime where it was derived. This accuracy suggests that the system may be described in a way that is manifestly homogeneous in Δ . However, we have not been able to find a simple theory of this type.

The main experimental implication of the theory above is that one should not expect to see a transition from a wrinkled to a folded state in a large experimental system. For overall displacements Δ of order λ this finding is implicit in the work of ref. [10]. The strain and the wrinkle amplitude at the threshold of their fold behavior goes to zero as the system size L goes to infinity. Nevertheless, our work shows that the transition to a strongly folded state, presented in ref. [10], is a smooth crossover, not a true transition. Even when the overall displacement Δ is indefinitely smaller than the wrinkling wavelength λ , the uniformly wrinkled state is unstable against a state of localized deformation.

Furthermore, if the assumption of incompressibility employed throughout our analysis is relaxed, another non-zero critical displacement appears, where a transition from the flat to a wrinkled state takes place. This buckling occurs at a displacement Δ_b where the in-plane compressional stress $Y(\Delta_b/L)$ (Y being the two-dimensional compression modulus of the sheet), exceeds the buckling stress of the sheet $2(BK)^{1/2}$. Now, if the system size L is sufficiently large, we will have $\Delta_c < \Delta_b$, and the regime of uniform wrinkling will disappear altogether. The condition for such a direct flat-to-fold transition [18] is $L \gtrsim (Y/K)^{1/2} \sim (Y/B)^{1/2} \lambda^2 \sim \lambda^2/t$, where we have used the scaling of the compression and bending moduli with the sheet thickness t : $Y \sim t$ and $B \sim t^3$. The inclusion of compressibility renders the transition first-order [16], in contrast to the continuous incompressible case treated by ref. [10] and in the present work.

The wrinkled state has not been observed in macroscopic Langmuir monolayers [9]. We believe that the theory above explains this lack of observation. In a typical Langmuir-monolayer experiment $L \sim 10$ cm and $\lambda \sim 1$ μ m. Hence, a wrinkled state should get localized already for extremely small displacements, $\Delta > \Delta_c \sim \lambda^2/L \sim$

0.1 \AA . The thickness of the monolayer is of 1 nm scale, implying the lack of extended wrinkling for $L \gtrsim 1$ cm. Thus, we expect that in such experiments there is a direct transition from flat to folded configurations. Because of the relevance of compressibility in this experiment, we expect the folds to form via discontinuous, abrupt events, as observed [5]. The wrinkled state *has* been reported experimentally [10,15] in systems that are not extremely large compared to λ . As discussed in the Appendix, the wrinkled state can be stable in systems where $L \lesssim \lambda^2/\Delta$. Other experiments exhibiting wrinkling [7] have strongly constrained lateral boundaries that likely form a barrier against folding.

The wrinkle-to-fold transition has been applied to describe not only fluid substrates but also elastic substrates of stiffness K . In the lowest-order approximation, these two situations are indeed equivalent. However, in the next-leading order treated here, the elastic system becomes different from the fluid system because an elastic substrate then exerts shear stresses on the sheet, while the fluid substrate does not. It may well be that the wrinkled state is more stable on an elastic substrate than on the liquid substrate treated above.

It is interesting to compare the present instability with that seen in an ordinary first-order transition near the spinodal line [19]. In this case as in ours, the leading-order contribution to the energy is stabilizing — favoring zero amplitude of the new phase. In both cases the next leading order is destabilizing. In both cases one may choose an intensive variable (*i.e.*, pressure) as the control parameter, or an extensive one (*i.e.*, volume or our displacement Δ). In the phase transition case, the current phase is metastable. A nonzero threshold volume of material must nucleate the new phase in order for the transition to occur. In the folding transition, there is likewise a critical displacement required for any pressure P below the threshold. As the control parameter moves to the spinodal line, the new phase dictated by the lowest-order energy begins to grow spontaneously. The counterpart of this behavior in our system would be for a wrinkled phase to grow in amplitude. However, the above analysis indicates a different behavior for the case of folding. Rather than growing in amplitude as dictated by the lowest-order energy, the wrinkled state collapses into a fold.

The enhanced localization arises because of the unexpected importance of non-leading energetic terms at indefinitely small Δ . An extended state, however small its amplitude, can be rearranged to produce a localized state of nonvanishing amplitude, for which nonleading contributions to the energy are significant. (As we noted, any uniform wrinkle must have vanishing amplitude and hence vanishing anharmonic energy.)

The localized buckling studied here resembles the buckling of a thick elastic film that is put under compressive strain [20,21]. In this case as in ours, linear response suggests an undulating surface. However, higher-order parts of the energy lead to a localized crease of nonzero slope but arbitrarily small depth. An analogous localized instability occurs in an elastic solid under tensile stress. Typical models of elastic solids are linearly unstable to the formation of

cavities of arbitrarily small size [22]. Our case differs from these two in that our localized state occupies a region of diverging size as the threshold is approached. This “progressive localization” bears closer resemblance to that seen in the nonlinear Schrödinger equation for wave-function ψ :

$$-\frac{\partial^2 \psi}{\partial x^2} - |\psi|^2 \psi = E\psi.$$

Here any negative energy E produces a localized bound state with a spatial extent that diverges as $E \rightarrow 0$ (albeit with no oscillation) [23].

Conclusion

The incipient folding instability described above opens several promising directions. The energy and incipient shape found here form the basis for predicting the time dependence of folding. The observed abrupt appearance and arrest of folds in time has long been a puzzle [5]. The unexpected simplicity of the energy versus displacement suggests an underlying symmetry of the system as yet undiscovered. Our work on these problems is in progress.

The authors warmly acknowledge insightful discussions with Ka Yee Lee, Luka Pocivavsek, Jin Wang, Enrique Cerda, and Benny Davidovitch. This work was completed at the Aspen Center for Physics. It was supported in part by the US-Israel Binational Science Foundation under Grant Number 2006076, and in part by the National Science Foundation’s MRSEC Program under Award Number DMR 0820054.

Appendix A. Finite-size effect

The analyses in sects. 3 and 4 have been restricted to the limit of a very large system size, $1 \ll \kappa^{-1} \ll L$. However, above and sufficiently close to the wrinkle-to-fold transition (*i.e.*, for $\Delta \gtrsim \Delta_c = 48/L$), κ is arbitrarily small, and the assumption $\kappa L \gg 1$ must break down. We now treat this limit of very small displacement, where $(\kappa^{-1}, L) \gg 1$ but κL may be finite.

For such minute deformations an ‘evanescent wave’ *Ansatz*,

$$h(s) = A \sin(ks) e^{-\kappa|s|}, \quad (\text{A.1})$$

gives the correct qualitative behavior as regards the scaling laws while simplifying the required integrations. An odd function has been chosen in eq. (A.1) to avoid a divergent curvature at $s = 0$. We set $k = k_c = 1$ and $L = 2\pi n$, where n is a large integer (*i.e.*, the system size is compatible with a large integer number of wrinkling wavelengths). We repeat the same procedure from sect. 4 — substitute eq. (A.1) in eq. (2), calculate E and Δ to second order in A^2 , express A^2 as a function of Δ , and substitute it back in the energy to get $E(\Delta)$. There are two differences in the current calculation: (a) the integrations in eq. (2) are performed over the finite interval $(-L/2, L/2)$ rather than an

infinite one; (b) we expand the expressions in small κ but keep terms that include κL intact. The resulting energy is

$$E = 2(1 + 2\kappa^2)\Delta - \frac{1}{2}\kappa \coth\left(\frac{\kappa L}{2}\right) \Delta^2. \quad (\text{A.2})$$

Minimization of E with respect to κ yields the following equation:

$$\kappa L = \frac{\Delta L}{16} f(\kappa L), \quad f(x) = \frac{\sinh x - x}{\cosh x - 1}. \quad (\text{A.3})$$

For $\Delta < \Delta_c = 48/L$ this equation has only the trivial solution, $\kappa = 0$, corresponding to the wrinkled state. For $\Delta > \Delta_c$ a solution of finite κ appears, increasing continuously from zero and corresponding to the folded state. Thus, sufficiently close to the transition we may expand eq. (A.2) in small κ to get

$$E \simeq E_0 + 4\Delta(1 - \Delta/\Delta_c)\kappa^2 + (L^3\Delta^2/720)\kappa^4, \quad (\text{A.4})$$

where $E_0 = 2\Delta - \Delta^2/L$. This Landau-like energy makes evident the second-order nature of the transition, κ serving as the order parameter. From eq. (A.4) we obtain

$$\begin{aligned} \kappa &\sim \begin{cases} 0, & \Delta < \Delta_c \\ L^{-1}\Delta^{-1/2}(\Delta - \Delta_c)^{1/2}, & \Delta \gtrsim \Delta_c \end{cases} \\ E - E_0 &\sim \begin{cases} 0, & \Delta < \Delta_c \\ -L^{-1}(\Delta - \Delta_c)^2, & \Delta \gtrsim \Delta_c. \end{cases} \end{aligned} \quad (\text{A.5})$$

At $\Delta = \Delta_c$ there is a discontinuous jump in $d^2E/d\Delta^2 = dP/d\Delta$.

References

1. N. Bowden, S. Brittain, A. G. Evans, J. W. Hutchinson, G. W. Whitesides, *Nature* **393**, 146 (1998).
2. E. Sharon, B. Roman, M. Marder, G. Shin, H. Swinney, *Nature* **419**, 579 (2002).
3. E. Cerda, L. Mahadevan, *Phys. Rev. Lett.* **90**, 074302 (2003).
4. E. Cerda, L. Mahadevan, J. Pasini, *Proc. Natl. Acad. Sci. USA*, **101**, 1806 (2004).
5. A. Gopal, V. Belyi, H. Diamant, T. A. Witten, K. Y. C. Lee, *J. Phys. Chem. B* **110**, 10220 (2006).
6. T. A. Witten, *Rev. Mod. Phys.* **79**, 643 (2007).
7. J. Huang, M. Juskiewicz, W. H. de Jeu, E. Cerda, T. Emrick, N. Menon, T. P. Russell, *Science* **317**, 650 (2007).
8. B. Audoly, A. Boudaoud, *J. Mech. Phys. Solids* **56**, 2444 (2008).
9. K. Y. C. Lee, *Ann. Rev. Phys. Chem.* **59**, 771 (2008).
10. L. Pocivavsek, R. Dellsy, A. Kern, S. Johnson, B. Lin, K. Y. C. Lee, E. Cerda, *Science* **320**, 912 (2008).
11. C. Py, P. Reverdy, L. Doppler, J. Bico, B. Roman, C. N. Baroud, *Eur. Phys. J. Special Topics* **166**, 67 (2009).
12. B. Davidovitch, *Phys. Rev. E* **80**, 025202 (2009).
13. J. Huang, B. Davidovitch, C. D. Santangelo, T. P. Russell, N. Menon, *Phys. Rev. Lett.* **105**, 038302 (2010).
14. D. P. Holmes, A. J. Crosby, *Phys. Rev. Lett.* **105**, 038303 (2010).

15. B. D. Leahy, L. Pocivavsek, M. Meron, K. L. Lam, D. Salas, P. J. Viccaro, K. Y. C. Lee, B. Lin, *Phys. Rev. Lett.* **105**, 058301 (2010).
16. L. D. Landau, L. M. Lifshitz, *Theory of Elasticity* (Pergamon, New York, 1986).
17. S. T. Milner, J.-F. Joanny, and P. Pincus, *Europhys. Lett.* **9**, 495 (1989).
18. Q. Zhang and T. A. Witten, *Phys. Rev. E* **76**, 041608 (2007).
19. H. E. Stanley, *Introduction to Phase Transitions and Critical Phenomena* (Oxford University Press, New York, 1987).
20. J. Kim, J. Yoon, R. C. Hayward, *Nat. Mater.* **9**, 159 (2010).
21. E. Hohlfeld, L. Mahadevan, e-print arXiv:1008.0694, 2010.
22. J. Sivaloganathan, S. J. Spector, *J. Elasticity* **93**, 177 (2008).
23. C. Pethick, *Bose-Einstein Condensation in Dilute Gases* (Cambridge University Press, New York, 2008).